

Membrane Metasurfaces

Quanlong Yang^{1,*}, Sergey Kruk¹, Yuehong Xu², Qingwei Wang², Yogesh Kumar Srivastava^{3,4}, Kirill Koshelev¹, Ivan Kravchenko⁵, Ranjan Singh^{3,4}, Jiaguang Han², Yuri Kivshar¹, and Ilya Shadrivov¹

¹Nonlinear Physics Centre, Australian National University, Canberra ACT 2601, Australia

²Center for Terahertz Waves, Tianjin University, Tianjin 300072, China

³Division of Physics and Applied Physics, School of Physical and Mathematical Sciences, Nanyang Technological University, Singapore 637371, Singapore

⁴Centre for Disruptive Photonic Technologies, The Photonics Institute, Nanyang Technological University, Singapore 637371, Singapore

⁵Center for Nanophase Materials Sciences, Oak Ridge National Laboratory, TN 37831, USA

*E-mail address: Quanlong.Yang@anu.edu.au

Abstract: We introduce a Mie-resonant membrane metasurface for THz frequency. The 2π phase coverage and high efficiency of membrane metasurface provide a novel opportunities for efficient wavefront control. The silicon membrane also supports the multifunctional metasurface. © 2019

The Author(s)

OCIS codes: (290.4020) Mie theory; (160.3918) Metamaterials; (050.6624) Subwavelength structure

1. Introduction

Metasurfaces with planar subwavelength resonators have been established as a highly flexible route to manipulate electromagnetic waves, including phase, amplitude, polarization and momentum. Dielectric metasurfaces supporting Mie-like resonances offer a significant advantage due to their low intrinsic material loss, promising various high-efficiency devices for flat optics. Magnetic and electric Mie-resonant multipoles play a crucial role in controlling the interference and scattering of light. Especially, with spectrally overlapped magnetic and electric multipoles, Huygens' metasurfaces allow light-wave manipulation with close to 100% transmission efficiency and a complete 2π phase coverage [1]. By tuning the interference of electric and magnetic multipole scatterings, dielectric metasurfaces enable almost arbitrary complex wave-front shaping and polarization manipulation.

For the typical dielectric metasurface made of high-index dielectric resonators placed on a low-index substrate, the overall efficiency of such resonators is affected by the contrast of refractive indices of the resonator and substrate materials. To eliminate the limitation of the substrate, by inverting the standard design of Mie resonators, we introduce and realize experimentally a free-standing membrane metasurface consisting of arrays of holes made in a thin silicon membrane at terahertz frequency [2]. It resembles a photonic-crystal slab, except that the periodicity is deeply subwavelength and Mie-type resonances define its functionalities [3]. As we demonstrated, the membrane metasurface can exhibit high transmission and 2π phase coverage. We compare the response of the membrane metasurface to that of the conventional Huygens' metasurface created by individual dielectric resonators, and we reveal their close correspondence. By inverting the structure from disks to holes, we interchange the mutual positions of the electric and magnetic resonances, and this resembles the Babinet principle for perfect conducting screens. Our further demonstration of wavefront control establishes a flexible and efficient platform for efficient photonic devices.

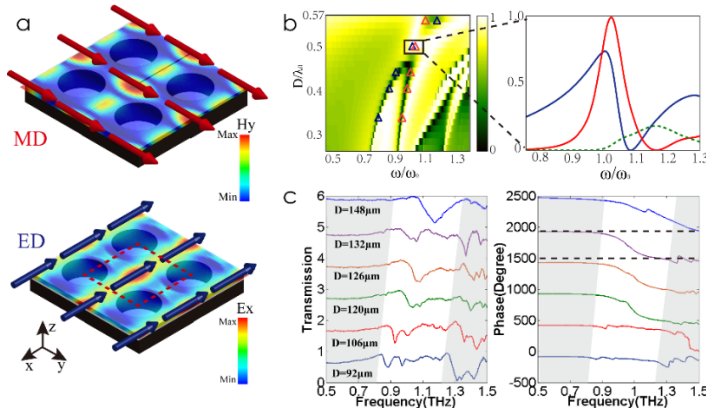


Fig. 1. Mode analysis and transmission performance of membrane metasurface. (a) The field distribution of magnetic dipole (MD, red arrows) and electric dipole (ED, blue arrows) of membrane metasurface. The thickness is $h = 50 \mu\text{m}$ and the period is $P = 158 \mu\text{m}$. (b) The transmission spectrum of the silicon membrane versus the diameter of holes. The red and blue triangles represent the MD and ED frequencies, respectively. Here, ω_0 and λ_0 represent the target frequency and wavelength. Enlarged image is the total multipole contributions of ED, MD resonances, and sum of high order multipoles (HOM). (c) Measured transmission and phase profile of the membrane metasurfaces.

2. Results and Discussions

In Fig. 1(a), we extract the transmission spectra and field profiles of the Mie resonances from the finite-element numerical analysis, and calculate the electric and magnetic dipole contributions to the total scattering cross-section for silicon membrane, by applying the multipole decomposition. Two ED and MD modes of the membrane metasurface are positioned in-between the holes, which are denoted by the blue and red arrows, respectively. We find that in both cases the optical response is dominated by the electric and magnetic Mie-type dipole resonances with smaller contributions from higher-order multipole modes [Fig. 1(b)]. Two transmission minima match well with the position of the ED and MD resonances. When increasing the diameter, we identify ED and MD resonances overlapping at a specific critical diameter and separated for either larger or smaller diameters. For the silicon membrane, the dipole resonances can be brought into a spectral overlap (at $D = 132 \mu\text{m}$), see Fig. 1(b). Next, we study the membrane metasurfaces experimentally. A standard photolithography defines the pattern, and a deep reactive ion etching is used to perforate the wafer. The measured transmission and phase profiles agree well with the theoretical and simulation results, see Fig. 1(c). In our experiments, the transmission of the metasurfaces reached 84.7%.

To demonstrate the wavefront control of membrane metasurface, we design a metalens with a hyperbolic phase profile, and the design focal length is 12 mm [see Fig. 2(a)]. We observe an excellent agreement between the numerically simulated results and experimentally measured data [see Figs. 2(b, c)], which clearly illustrates the beam focusing.

Furthermore, we realize a multifunctional membrane metasurface that can switch its functionality from a magnetic mirror to a Huygens' surface by altering the incident polarization. The inset of Fig. 2(d) shows the SEM image of the fabricated metasurface. Here, the short and long axes of the elliptical holes are set to $D_1 = 118 \mu\text{m}$ and $D_2 = 132 \mu\text{m}$, respectively. In Fig. 2(d), we identify two transmission minima close to zero for TE polarization. For TM, the transmission amplitudes will increase to 0.83 and 0.90, respectively.

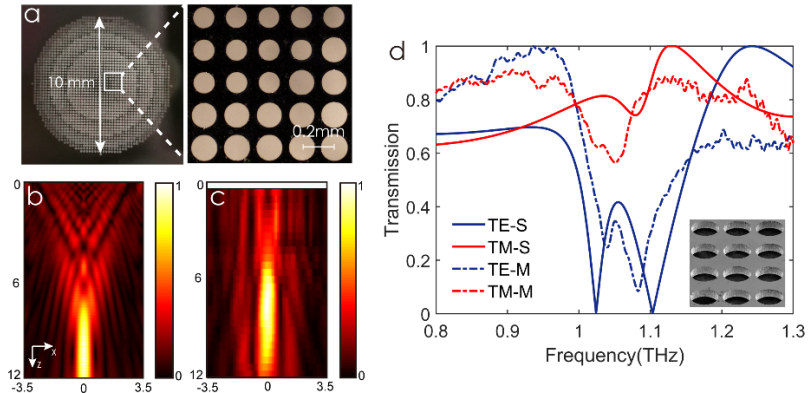


Fig. 2. Demonstration of membrane metasurface for wavefront control. (a) Optical image of designed metalens based on a silicon membrane. (b, c) Numerically simulated and experimentally measured electric field distribution of the membrane metasurface. The units are mm. (d) Simulated (solid) and measured (dash) transmission amplitude of multifunctional metasurface under TE and TM incidence. The inset is the SEM image of the fabricated sample.

3. Conclusions

We suggested a novel approach for efficient all-dielectric membrane Huygens' metasurfaces. We identified the condition for overlapping the electric and magnetic resonances in the membrane metasurface for achieving highly efficient transmission and 2π phase coverage. The demonstration of wavefront control and multifunctional metasurface proves the potential for flat-optic devices.

Acknowledgments. The authors acknowledge the use of the Australian National Fabrication Facility (ANFF), the ACT Node. The work has been supported by the Australian Research Council and the Strategic Fund of the Australian National University. A portion of his research was conducted at the Center for Nanophase Materials Sciences, which is a DOE Office of Science User Facility.

4. References

- [1] M. Decker, I. Staude, M. Falkner, J. Dominguez, D. Neshev, I. Brener, T. Pertsch, and Y. Kivshar, "High-efficiency dielectric Huygens' surfaces", *Adv. Opt. Mater.* **3**, 813-820 (2015).
- [2] Q. Yang, S. Kruk, Y. Xu, Q. Wang, Y. Srivastava, K. Koshelev, I. Kravchenko, R. Singh, J. Han, Y. Kivshar, and I. Shadrivov, "Mie-Resonant Membrane Huygens' Metasurfaces", *Adv. Func. Mater.* **30**, 1906851 (2020).
- [3] W. Zhao, W. Yang, and C. Chang-Hasnain, "Progress in 2D photonic crystal Fano resonance photonics", *Progress in Quantum Electronics*

38, 1-74 (2014).